La0.8Pb0.1Ca0.1Fe1–xCoxO3 thin films as ozone-sensitive layers

S. Smiy, M. Bejar, E. Dhahri, T. Fiorido, K. Aguir, Marc Bendahan

$La_{0.8}Pb_{0.1}Ca_{0.1}Fe_{1-x}Co_xO_3$ $(0.00 \leq x \leq 0.20)$ thin films-as ozone sensitive layers

S. Smiy [a,*], M. Bejar [a] , E. Dhahri [a], T. Fiorido [b], K. Aguir [b], M. Bendahan [b]

[a] *Laboratoire de Physique Appliquée, Faculté des Sciences, B.P. 1171, 3000 Sfax, Université de Sfax, Tunisie.*

[b] *Aix Marseille Univ, Université de Toulon, CNRS, IM2NP, Marseille, France 13013*.

ABSTRACT

This paper describes the realization and characterization of $La_{0.8}Pb_{0.1}Ca_{0.1}Fe_{1-x}Co_xO_3$ gas-based sensors. $La_{0.8}Pb_{0.1}Ca_{0.1}Fe_{1-x}Co_xO_3$ $(0.00 \leq x \leq 0.20)$ thin films were preparing using the drop-coating method over a Si/SiO_2 substrate with inter-digitated Pt-electrodes. The sensors thus produced exhibit a good sensitivity to ozone at low concentration. The substitution of iron atoms by cobalt ones increases the sensor responses "S", from 1.716 for $x = 0.00$ to 6.584 to $x = 0.20$ for an ozone concentration equal to 400 ppb. In addition, the substitution of iron by cobalt induces a decrease in the sensor operating temperature from 270 $°C$ for the parent compound ($x = 0.00$) to 170 $°C$ for $x = 0.20$.

Keywords: Perovskites, Drop coating, Co-doped, Thin films, Sensors, Ozone, $sub-ppm$.

Corresponding author: sabsmiy@gmail.com ($S. Smiy$)

I- INTRODUCTION

Perovskite materials exhibit interesting physicochemical properties which make them promising for gas detection applications. $LaFeO_3$, the mother compound has been found to be a good candidate for NO_2 [1], formaldehyde [2], acetone [3], ethanol [4] and NH_3 detection [5] *etc*. To develop the detection properties of this functional material, it is necessary to perform numerous substitutions in the La and Fe sites in order to increase the response of these sensors [6 - 8]. The need for ozone sensors is increasing in the fields, *of* textile, food, water treatment, pharmaceutical products and the purification of gases [9]. The exposure to ozone at concentrations greater than 120 ppb can cause serious health problems (eye irritation, lung damage and respiratory irritation). Moreover, the air quality can be classified referring to the Ozone amount in the atmosphere, as very good

$(0 - 50\,ppb)$ and poor $(C > 50\,ppb)$ [9]. In this respect, the Ozone concentration monitoring in our atmosphere is becoming a serious issue [7, 8]. Recently, several attempts have been made to the development of new materials devoted to ozone gas sensing. In particular, M. Mori et *al*. have found that introducing Co in place of Fe increases the response of $SmFeO_3$ and $SmFe_{0.9}Co_{0.1}O_3$ sensor and the results showed that the substitution of Fe by Co was accompanied by a decrease in the sensor operating temperature [10].

There are many interests in perovskite structured compounds (with general formula ABO_3) due to their colossal magnetoresistance effects [11], their unique catalytic action [12] and their gas sensing applications [13]. Ferrite $LaFeO_3$ materials have a great effect on technological development and are widely used in various domains, such as magnetic refrigeration and gas sensing application. The structural characteristics of these compounds can lead to a range of useful physical properties, such as mixed electric, ionic conductivity and ordered magnetism at elevated temperature. While at present, most of the studied perovskites related oxide compounds, such as the rare earth strontium cobaltates, have been investigated for use as cathode materials for solid oxide fuel cells SOFC, magnetic sensors and for high temperature oxygen separation [14]. Furthermore, it has been reported that $LaFeO_3$ (LFO) compound is characterized by higher resistance, which presents a disadvantage for the gas sensing application. In this regard, it has also been reported that the partial substitution of La by lower valent cation elements such as Pb [15] and Ca [16] can reduce the resistance of the (LFO) compound. Moreover, and using Kroger-Vink defect notations, its charge carries are holes $h^{\cdot}$, which are produced by the ionization of La^{3+} ions vacancy defect $[V_{La}^{x}]$ and the ionization reaction is $(V_{La}^{x} \rightarrow V_{La}^{'''} + 3h^{\cdot})$. When La^{3+} is substituted by Pb^{2+}, the ionization reaction of this element is $(Pb_{La}^{x} \rightarrow Pb_{La}^{'} + h^{\cdot})$ (where, Pb_{La}^{x} is related to the point defect formed when La^{3+} is replaced by Pb^{2+} in the crystal state and $h^{\cdot}$ are the generated holes). As a result of $[Pb_{La}^{x}] >>> [V_{La}^{x}]$, the mobility of holes increases, and consequently the resistance of the doped compound decreases compared to the (LFO) one [17].

In our previous published work related to this framework, we have demonstrated that introducing cobalt instead of Iron in $La_{0.885}Pb_{0.005}Ca_{0.11}Fe_{1-x}Co_xO_{2.95}$ $(x = 0.00, 0.05, 0.10$ and $0.15)$ compounds leads to the decrease of the operating temperature

from 270 °C for $x = 0.00$ to 250 °C for $x = 0.05$ in the presence of NH_3-gas [18]. In a related study H. Saoudi et *al*. have reported that introducing Cobalt instead of Iron in $La_{0.8}Pb_{0.1}Ca_{0.1}Fe_{1-x}Co_xO_3$ $(0.00 \leq x \leq 0.20)$ sensors using pellet forms increased the response in the presence of NH_3-gas compared to the mother compound $(x = 0.00)$[15]. Moreover, the responses of $La_{0.8}Pb_{0.1}Ca_{0.1}Fe_{1-x}Co_xO_3$ $(0.00 \leq x \leq 0.20)$ sensors found in this study were higher than the response of $La_{0.885}Pb_{0.005}Ca_{0.11}Fe_{1-x}Co_xO_{2.95}$ $(0.00 \leq x \leq 0.15)$ sensors found in our study [18, 19].

In parallel with our study and the study performed by H. Saoudi et *al.*, our contribution in this work aims to study the performance of $La_{0.8}Pb_{0.1}Ca_{0.1}Fe_{1-x}Co_xO_3$ $(0.00 \leq x \leq 0.20)$ compounds as an ozone sensor, for the first time, in the form of thin-film elaborated by the drop-coating method because, For this later application, the perovskite materials have been used in the pellet forms and have showed not enough sensitivity. Therefore, in order to increase their sensitivity, we considered that is necessary to deposit these materials, prepared by the sol gel method, by drop coating [20]. This choice is based on the fact that the sensitivity is directly related to the thickness of the used material.

II- Experimental details

II-1) Preparation of perovskites nano-powders and thin films deposition

The nanocrystalline $La_{0.8}Pb_{0.1}Ca_{0.1}Fe_{1-x}Co_xO_3$ $(0.00 \leq x \leq 0.20)$ powders have been prepared using the sol-gel method. The different precursors $La(NO_3)_3.6H_2O, Pb(NO_3)_2.2H_2O, Ca(NO_3)_2.4H_2O, Fe(NO_3)_3.9H_2O$ and $Co(NO_3)_2.6H_2O$ have been dissolved in distilled water at 70 °C. Then, the citric acid and the polyethylene glycol (PEG) were added to the mixture to achieve polymerization and well homogenization. Finally, the obtained powder has been sintered at 300, 600 and 900°C for one day for each temperature.

Nowadays, there are many methods which are used to develop sensors. In this paper we use the drop coating because it is a chemical method and in this context F.L. Pennec et. al [21] carried out a study about methods used in the elaboration of $BaTiO_3$ perovskite materials, authors mentioned that response is more important in case of Drop coating method compared to Screen printing method in presence of 400 ppm of CO_2 gas, added to that the recovery time in case of drop coating method is equal to 4min but in case of Screen printing method this time is found to be equal to 5min.

The deposition of the thin film over the Si/SiO_2 substrate with inter-digitated Pt-electrodes has been performed using the drop-coating method. The coating suspensions have been obtained by mixing 20 mg of powders from each compound with 20 $m\ell$ of 2-propanol, followed by 10 min ultrasonication at 40 °C for a good homogenization. The coating sample has been performed drop by drop over the substrate using a micropipette. The thin films were obtained after the deposition of 8 drops which correspond to 20 µℓ. The coating process has been followed by heating samples for 1 h at 500 °C.

Film thickness is measured after annealing using a DEKTAK 6M mechanical profilometer. Ten measurements are made at different locations and the average thickness is found as 300 nm.

In order to ensure the adsorption of our powder over the Si/SiO_2 substrate, a view of the deposited thin film has been carried out by an optical microscope with magnifications of 800 µm and 150 µm (Figure 1).

II-2) Ozone sensing measurements

Ozone-gas is generated using an UV lamp (Stable Ozone Generator UVP/185nm). Firstly, dry air is passed through a quartz tube. The light up of the UV lamp radiation transformed some of the oxygen molecules into O_3 (ozone). The intensity of the UV radiation has been varied by shifting a shutter around the lamp. The different ozone concentrations were obtained in the range of 50 ppb to 400 ppb with a dry air flow rate maintained at 0.5 ℓ / min. A heating source was used to regulate the operating temperature. The applied dc voltage for sensors measurement was fixed to 1 V and the resistance was controlled by a keithley 4250 sourcemeter (Figure 2 (a, b)).

III- RESULTS AND DISCUSSION

III-1) XRD and EDS Studies:

XRD patterns based on the use of $Cu - K_\alpha$ radiation source of the prepared nanopowders $La_{0.8}Pb_{0.1}Ca_{0.1}Fe_{1-x}Co_xO_3$ $(0.00 \leq x \leq 0.20)$ are used to identify the structure of our samples. The Rietveld refinement of the XRD patterns using the FullProf program, presented in Figure 3. (a), proves that all the samples are indexed in the orthorhombic system with $Pnma$ space group. Besides, the substitution of iron by cobalt leads to a decrease in cell-parameters and consequently the decrease of the volume (Figure 3. (b)). Moreover, the presence of other peaks characteristic of Fe_3O_4 secondary phase has been

identified in this study using "$X0$ Pert High Score Plus" program. This phase was found to crystallize in the orthorhombic structure with $Pbcm$ space group [9, 18]. The refinement parameters are gathered in Table 1.

The crystallite size of the prepared samples was calculated using the Williamson-Hall's equation $(W-H)$ [19] $(Eq.\,1)$:

$$\beta cos(\theta) = k\lambda/D_{W-H} + 4\varepsilon \sin(\theta) \qquad (Eq.\,1)$$

Where: θ is the Bragg diffraction angle, β defines the effective strain, k is the shape factor and the D_{W-H} presents the average crystallites size. The D_{W-H} of $La_{0.8}Pb_{0.1}Ca_{0.1}Fe_{1-x}Co_xO_3$ $(0.00 \leq x \leq 0.20)$ samples were obtained by the linear variation of $(\beta\cos(\theta)$ *vs.* $(4 * \sin(\theta))$ (Figure. 4). The D_{W-H} values, obtained from the intercept of the linear adjustment values, are regrouped in Table. 2. The results clearly indicate the decrease of the average crystallites size from 83.023 nm for $x = 0.00$ to 43.870 nm for $x = 0.20$. These values are close to those obtained with other compounds considered as nanometric materials for gas-sensing application [22 - 24]. "As an example we can cited that in our ancient article, crystallite size is found to be equal to 52.11 nm in case of $La_{0.885}Pb_{0.005}Ca_{0.11}FeO_{2.95}$ sensor which is used for NH_3 sensing application [22]. In addition A. Benali et al. mentioned that their samples $La_{0.8}Ca_{0.2-x}Pb_xFeO_{2.95}$ present a crystallites size included between 40.19 nm and 65.51 nm and usually nanocrystals with a smaller grain size had a higher activity, which could facilitates the chemisorption of oxygen [23].

Hence, the decrease of the nanometric crystallite size with increasing the cobalt content on prepared samples has been expected to increase the response.

The SEM micrographs of $La_{0.8}Pb_{0.1}Ca_{0.1}Fe_{1-x}Co_xO_3$ $(0.00 \leq x \leq 0.20)$ sensors confirm the homogeneous microstructure, with the presence of a porous character of the surface Figure. 5 (a). Moreover, the EDS-Mapping presented in Figures 5 (b, c) Shows the existence of all the elements introduced in our samples, particularly, $La, Pb, Ca, Fe, Co, and\ O$ [25].

III-2) Ozone sensing properties

$La_{0.8}Pb_{0.1}Ca_{0.1}Fe_{1-x}Co_xO_3$ $(0.00 \leq x \leq 0.20)$ sensing performances have been tested at different operating temperatures ranging from 160 °C to 280 °C in order to determine the

optimum operating temperature of each sensor (T_{op}). Ozone-gas has been injected for a concentration equal to $100\,ppb$. The gas sensing characteristics of $La_{0.8}Pb_{0.1}Ca_{0.1}Fe_{1-x}Co_xO_3$ ($x = 0.00$ and $x = 0.10$) films are shown in Figures. 6(a) and 6(b) at $200, 220, 250$ and $270\ °C$. The exposure time to ozone was 1 minute. Adsorbed oxygen molecules onto the surface of our *P*-type $La_{0.8}Pb_{0.1}Ca_{0.1}Fe_{1-x}Co_xO_3$ ($0.00 \leq x \leq 0.20$) semiconductors were ionized into species such as $O^-_{2(ads)}$, $O^-_{(ads)}$ and $O^{2-}_{(ads)}$ and these forms are dominated at $T > 150\ °C$ [22].

The sensor response was defined as $= R_a/R_g$; where R_a and R_g present the sensor-resistances in air and ozone-gas, respectively [23]. Sensor's responses (S) are depicted in Tables. 3. According to the result, it's evident that the highest responses were at $T_{op} = 270°C$ for the undoped sensor ($x = 0.00$) and at $T_{op} = 170\ °C$ for $x = 0.20$.

Figure. 7 depicts the variation of the operating temperatures as a function of Co-content. The results display that introducing cobalt (Co) instead of iron (Fe) increases the operating temperatures of the sensors. These findings are in agreement with those found by M. Mori and *al*. where the substitution of Fe by Co in $SmFe_{1-x}Co_xO_3$ compounds decreased the operating temperature from $290\ °C$ for $x = 0.00$ to $150\ °C$ for $x = 1.00$ in the presence of O_3-gas [10].

Furthermore, the sensing performances of our sensors have been tested for various ozone (O_3) concentrations. Figure. 8 shows the ozone sensing properties when sensors are exposed to different concentrations ($50 - 400\ ppb$) at the optimal operating temperature (T_{op}) during an ozone exposure time of $4\,min$. These results show a certain proportionality between the response and gas concentrations. In fact, the sensors have shown an increase of the resistance with increasing O_3- concentrations ranging from 50 to 400 ppb and when Co-content increases. Consequently, the increase of the resistance induced the increase of the response S (Figures. 9 and 10) that reaches a maximum of $S = 6.583$ for the concentration of 400 ppb for the sample with $x = 0.20$. On the contrary, the response has decreased to $S = 2.878$ for the sample with $x = 0.05$ at the same concentration. Moreover, the curves demonstrate the possibility of detecting the lowest limit of 50 ppb ($sub - ppm$) of ozone gas.

The performances of $La_{0.8}Pb_{0.1}Ca_{0.1}Fe_{1-x}Co_xO_3$ ($0.00 \leq x \leq 0.20$) compounds such as response, stability, response time, and recovery time are influenced by the quantity and

quality of oxygen adsorbed on the surface of our sensors [26]. On the surface, atmospheric oxygen can be adsorbed very easily, and atoms or molecules become chemisorbed ions O^- or O_2^-. The increase of the temperature causes the rise of the state of oxygen on the surface to undergo the reactions described in the Eq. 2 to Eq. 5 and this phenomenon was demonstrated theoretically using the SnO_2 model [27].

In this context, the thin films present an increase in hole concentration because when oxygen species are adsorbed in $La_{0.8}Pb_{0.1}Ca_{0.1}Fe_{1-x}Co_xO_3$ $(0.00 \leq x \leq 0.20)$ materials, which are *p*-type semiconductors, a depletion region of electrons was formed [28].

$$O_{2(gas)} \leftrightarrow O_{2(ads)} \quad (Eq.2)$$

$$O_{2(ads)} + e^- \leftrightarrow O_{2(ads)}^- \quad (Eq.3)$$

$$O_{2(ads)}^- + e^- \leftrightarrow 2O_{ads}^- \quad (Eq.4)$$

$$O_{(ads)}^- + e^- \leftrightarrow O_{(ads)}^{2-} \quad (Eq.5)$$

The chemical reactions process between free adsorption site *S* and the triatomic gases, as Ozone (O_3), are illustrated according to the following reactions [29]:

$$S + O_3 \rightarrow (S-O) + O_2 \quad (Eq.6)$$

$$(S-O) + e^- \rightarrow (S+O)^- \quad (Eq.7)$$

The sensing responses $(S = R_a/R_g)$ of $La_{0.8}Pb_{0.1}Ca_{0.1}Fe_{1-x}Co_xO_3$ $(0.00 \leq x \leq 0.20)$ thin-films exposed to various concentrations of ozone were compared to those of several materials such as metal-oxide-semiconductor [30] and other perovskite materials [10, 31]. As seen in Table 4, our sensors present a higher response compared to other materials in all ranges of ozone concentrations. Furthermore, $La_{0.8}Pb_{0.1}Ca_{0.1}Fe_{1-x}Co_xO_3$ $(0.00 \leq x \leq 0.20)$ sensors are considered as $sub-ppm$ since the responses in the presence of 50 ppb were significantly better than those found by the other sensors [10, 31-38].

Commonly, the response time defined is the time needed to reach 90 % of saturation, whereas the recovery time is the time needed to recover 10 % of the original resistance [39]. The study of the response and recovery times for our $La_{0.8}Pb_{0.1}Ca_{0.1}Fe_{1-x}Co_xO_3$ $(0.00 \leq x \leq 0.20)$ thin films indicate significant values compared to other materials considered as potential gas sensors [40-42]. The values of response(τ_{resp}) and recovery (τ_{rec}) times of our compounds are gathered in Table 5. It's clear that curves do not return perfectly to the base line which gives an uncertainty on τ_{rec} values but we put the recovery

time in order to compare our values with those determined for other materials used in films forms for the detection of harmful gases.

IV- CONCLUSION

In this research paper, the ozone-sensing properties of $La_{0.8}Pb_{0.1}Ca_{0.1}Fe_{1-x}Co_xO_3$ $(0.00 \leq x \leq 0.20)$ thin films prepared by the drop-coating method have been investigated. The prepared sensors have demonstrated a good sensing performance. The results have shown that introducing cobalt instead of iron increased the response to O_3-gas and decreased the operating temperature from 270 $°C$ for $x = 0.00$ to 170$°C$ for $x = 0.20$. Moreover, all the prepared compounds displayed a $sub - ppm$ behavior. The studied samples, potentially, detected a lower limit of 50 ppb of ozone with high values of response and were $S = 1.025$, 1.110, 1.586 and 1.753 for $x = 0.00$, 0.05, 0.10 and 0.20, respectively. The finding confirms that the performances of the prepared thin films are a promising material for O_3 sensing applications. Further works will be extended to test other oxidizing gases such as NO_2 in order to evaluate the selectivity of these sensors towards ozone gas.

Table 1: The Rietveld refinement results of X-Ray diffraction (XRD) data of $La_{0.8}Pb_{0.1}Ca_{0.1}Fe_{1-x}Co_xO_3$ ($x = 0.00, 0.05, 0.10$ and 0.20) compounds.

x	0.00	0.05	0.10	0.20
Space group	$Pnma$	$Pnma$	$Pnma$	$Pnma$
a (Å)	5.549_3	5.543_1	5.534_2	5.518_2
$b/\sqrt{2}$ (Å)	5.550_0	5.539_0	5.527_7	5.513_7
c (Å)	5.539_4	5.535_1	5.528_3	5.506_5
V (Å^3)	60.314_0	59.301_2	59.792_2	59.234_0

Table 2: Values of D_{W-H} determined by Williamson-Hall method for $La_{0.8}Pb_{0.1}Ca_{0.1}Fe_{1-x}Co_xO_3$ ($x = 0.00, 0.05, 0.10$ and 0.20) samples.

x	$D_{W-H}(nm)$
0.00	83.023
0.05	75.231
0.10	52.436
0.20	43.870

Table 3: The relationship between response $(S = R_a/R_g)$ and temperature (T) of $La_{0.8}Pb_{0.1}Ca_{0.1}Fe_{1-x}Co_xO_3$ $(x = 0.00, 0.05, 0.10 \text{ and } 0.20)$ based sensors during ozone exposing time of *1 min* for a concentration equal to $100ppb$.

$x = 0.00$

$T\ (°C)$	$S(R_a/R_g)$	$T\ (°C)$	$S(R_a/R_g)$
200	1.018	**250**	1.017
210	1.019	**260**	1.017
220	1.016	**270**	**1.022**
230	1.013	**280**	1.019
240	1.013		

$x = 0.05$

$T(°C)$	$S(R_a/R_g)$	$T(°C)$	$S(R_a/R_g)$
200	1.042	**250**	**1.064**
210	1.050	**260**	1 ,051
220	1.052	**270**	1.051
230	1.051	**280**	1.028
240	1.056		

$x = 0.10$

$T(°C)$	$S(R_a/R_g)$	$T(°C)$	$S(R_a/R_g)$
180	1.201	**240**	1.160
190	**1.290**	**250**	1.143
200	1.254	**260**	1.140
210	1.231	**270**	1.152
220	1.191	**280**	1.198
230	1.168		

$x = 0.20$

$T(°C)$	$S(R_a/R_g)$	$T(°C)$	$S(R_a/R_g)$
160	1.330	**230**	1.160
170	**1.345**	**240**	1.155
180	1.171	**250**	1.153
190	1.237	**260**	1,139
200	1.220	**270**	1,132
210	1.183	**280**	1,157
220	1.211		

Table 4: Response values $(S = R_a/R_g)$ of $La_{0.8}Pb_{0.1}Ca_{0.1}Fe_{1-x}Co_xO_3$ $(x = 0.00, 0.05, 0.10\ and\ 0.20)$ sensors during ozone exposing time of 4 min (Present work : P.W) compared to others materials considered for O_3 sensing application.

Sensors	*T (°C)*	*C (ppb)*	*S*	References
$SrTi_{0.925}Fe_{0.075}O_3$	250	75	3	[25]
WO_3	300	50	1.25	[26]
SnO_3	523	50	3	[27]
$La_{0.8}Pb_{0.1}Ca_{0.1}FeO_3$	270	50	1.025	*P.W*
$La_{0.8}Pb_{0.1}Ca_{0.1}Fe_{0.9}Co_{0.1}O_3$	190	50	1.586	*P.W*
$La_{0.8}Pb_{0.1}Ca_{0.1}Fe_{0.8}Co_{0.2}O_3$	170	50	1.753	*P.W*
WO_3	300	100	1.42	[28]
WO_3	300	150	1.78	[28]
In_2O_3	473	100	1.5	[25]
$La_{0.8}Pb_{0.1}Ca_{0.1}FeO_3$	270	100	1.068	*P.W*
$La_{0.8}Pb_{0.1}Ca_{0.1}Fe_{0.9}Co_{01}O_3$	190	100	2.020	*P.W*
$La_{0.8}Pb_{0.1}Ca_{0.1}Fe_{0.8}Co_{0.2}O_3$	170	100	2.111	*P.W*
WO_3 *(EG : 50µm)*	250	200	1.7	[29]
$La_{0.8}Pb_{0.1}Ca_{0.1}FeO_3$	270	200	1.373	*P.W*
$La_{0.8}Pb_{0.1}Ca_{0.1}Fe_{0.9}Co_{0.1}O_3$	190	200	2.475	*P.W*
$La_{0.8}Pb_{0.1}Ca_{0.1}Fe_{0.8}Co_{0.2}O_3$	170	200	3.264	*P.W*
$SmFe_{0.8}Co_{0.2}O_3$	200	400	3	[10]
WO_3 *(EG : 50µm)*	250	400	2.3	[29]
$La_{0.8}Pb_{0.1}Ca_{0.1}FeO_3$	270	400	1.716	*P.W*
$La_{0.8}Pb_{0.1}Ca_{0.1}Fe_{0.9}Co_{0.1}O_3$	190	400	3.391	*P.W*
$La_{0.8}Pb_{0.1}Ca_{0.1}Fe_{0.8}Co_{0.2}O_3$	170	400	6.563	*P.W*
WO_3 *(EG : 50µm)*	250	800	2.8	[29]
In_2O_3	473	1000	2	[25]

Table 5: Response (τ_{resp}) and recovery (τ_{rec}) times of $La_{0.8}Pb_{0.1}Ca_{0.1}Fe_{1-x}Co_xO_3$ $(x = 0.00, 0.05, 0.10\ and\ 0.20)$ sensors at different concentrations (C) at the operating temperature for each sensor.

Sensors	$T_F\ (°C)$	Detected gas	$C\ (ppb)$	$\tau_{rep}\ (min)$	$\tau_{rec}\ (min)$	References
$x = 0.00$	270	O_3	50	3.4	2.5	*P.W*
$x = 0.00$	270	O_3	400	2.6	12.5	*P.W*
$x = 0.05$	250	O_3	50	3.38	13.2	*P.W*
$x = 0.05$	250	O_3	400	1.98	25.1	*P.W*
$x = 0.10$	190	O_3	50	3.30	10.2	*P.W*
$x = 0.10$	190	O_3	400	1.95	30.1	*P.W*
$x = 0.20$	170	O_3	50	3.51	8.3	*P.W*
$x = 0.20$	170	O_3	400	2.1	41.3	*P.W*
$SmFeO_3$	200	O_3	50	8.4	-	[31]
$SmFeO_3$	200	O_3	500	4.0	-	[31]
NiO	200	NH_3	1000 (ppm)	4.6	13	[32]
Pt/NiO	200	NH_3	200 (ppm)	6.6	120	[33]
Pt/NiO	200	NH_3	35 (ppm)	13.3	90	[33]

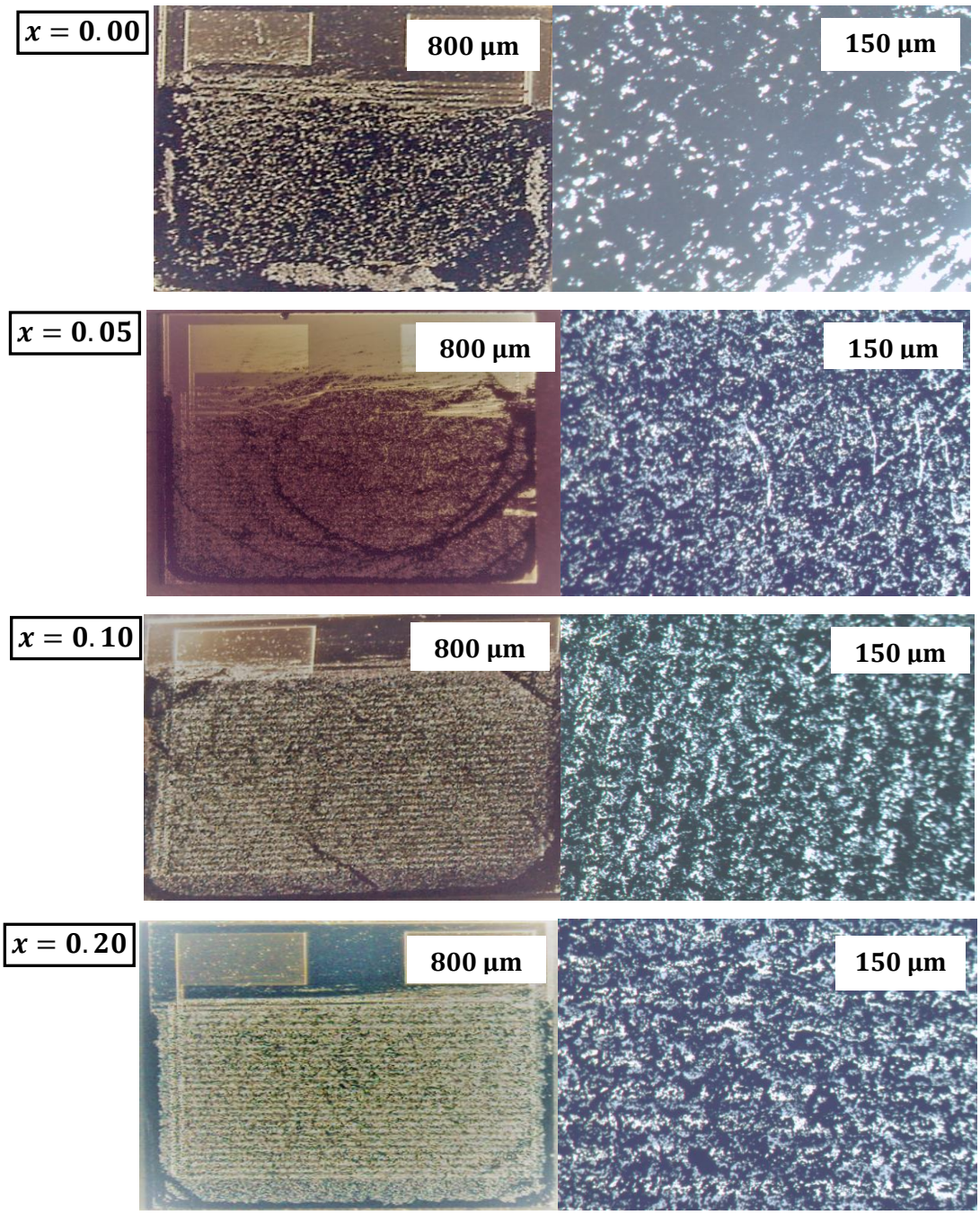

Figure 1: Optical view after drop coating of $La_{0.8}Pb_{0.1}Ca_{0.1}Fe_{1-x}Co_xO_3$ $(0.00 \leq x \leq 0.20)$ sensors of a magnifications equal to 800 µm and 150 µm.

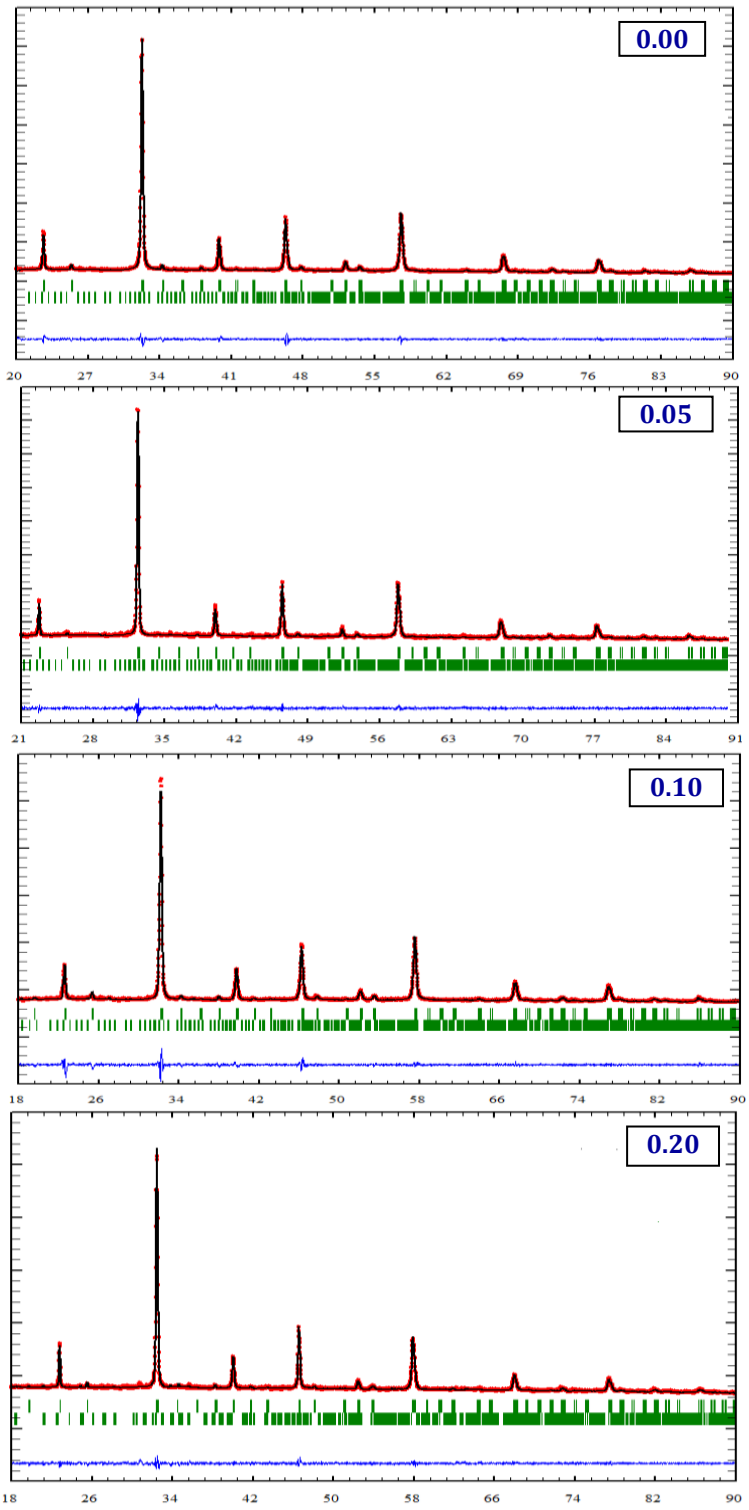

Figure 2 (*a*) : Observed (red), Calculated (black solid line), their difference patterns (blue) and the Bragg positions (green) of $La_{0.8}Pb_{0.1}Ca_{0.1}Fe_{1-x}Co_xO_3$ ($0.00 \leq x \leq 0.20$) sensors and the secondary phase which is attached to the Fe_3O_4 impurity.

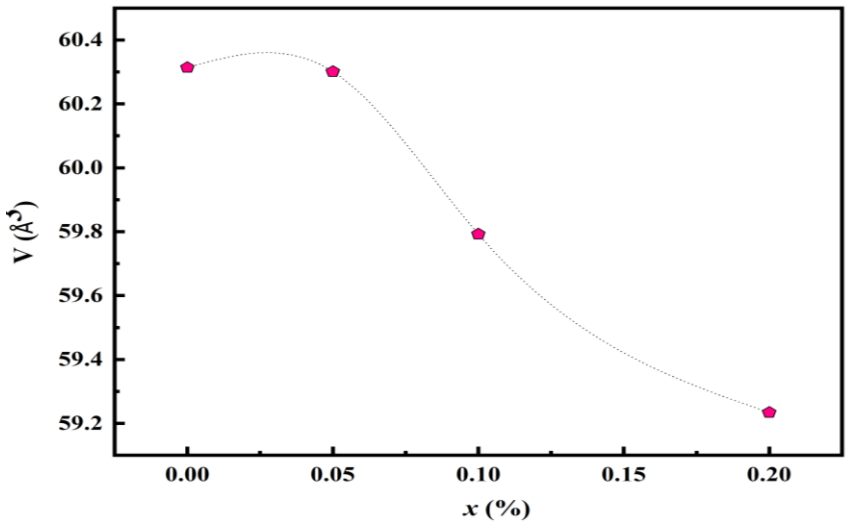

Figure. 2(*b*) : The unit cell volume as a function of cobalt content (x) of $La_{0.8}Pb_{0.1}Ca_{0.1}Fe_{1-x}Co_xO_3$ ($0.00 \leq x \leq 0.20$) compounds.

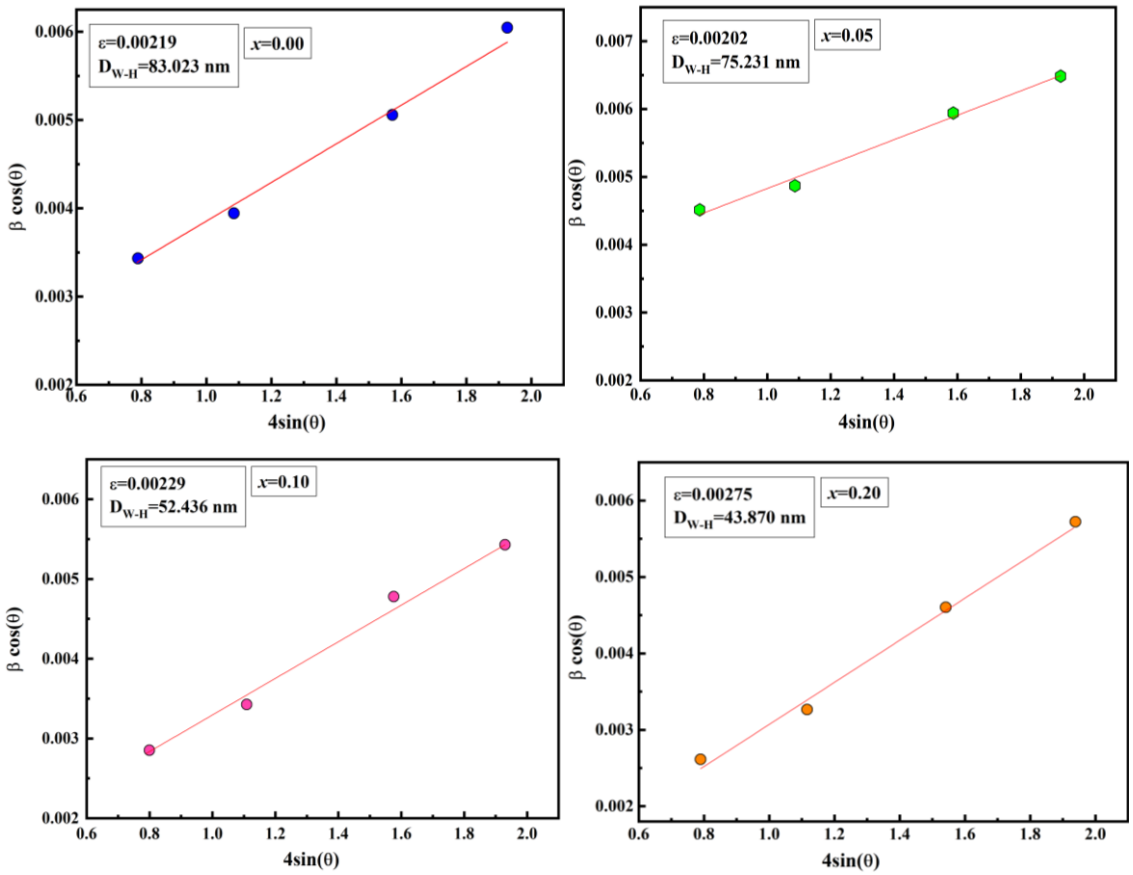

Figure. 3 : Williamson-Hall plots of $La_{0.8}Pb_{0.1}Ca_{0.1}Fe_{1-x}Co_xO_3$ $(0.00 \leq x \leq 0.20)$ nanopowders prepared by the sol-gel method.

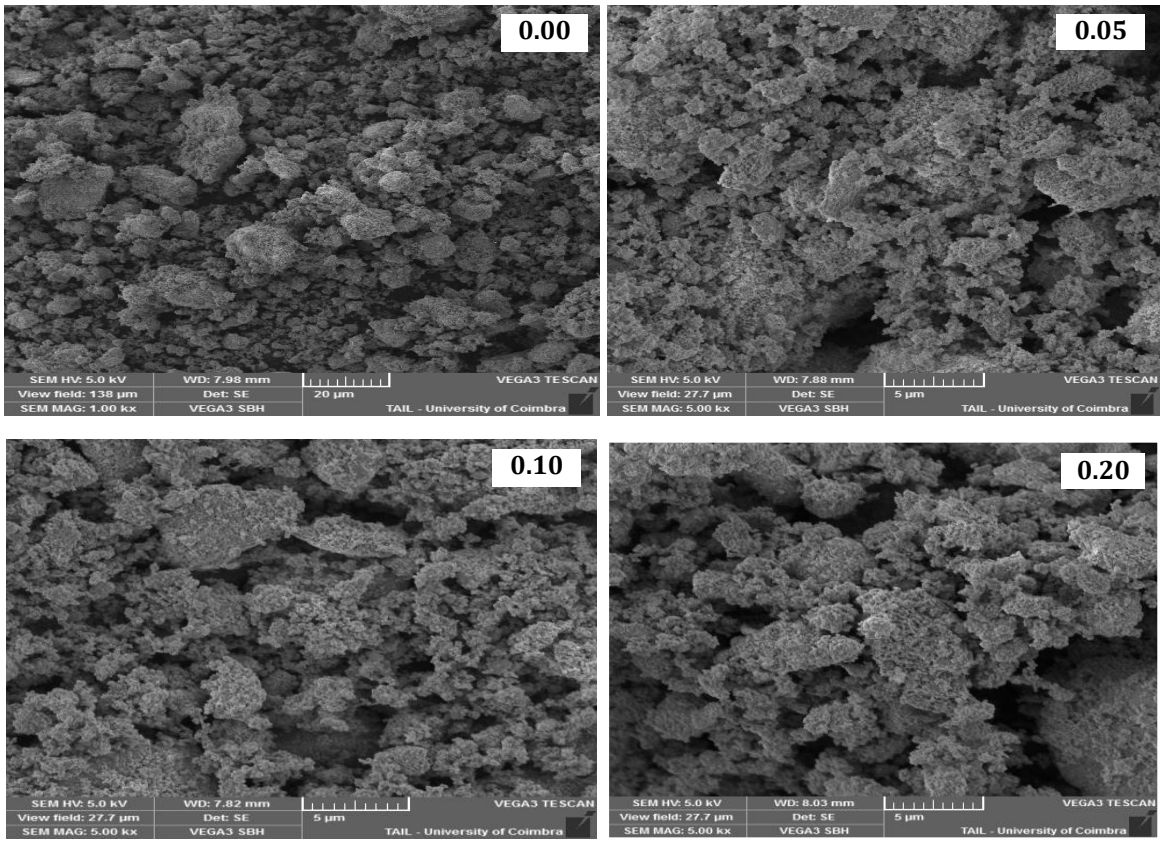

Figure. 4 (*a*) : *SEM*-graphs of $La_{0.8}Pb_{0.1}Ca_{0.1}Fe_{1-x}Co_xO_3$ $(0.00 \leq x \leq 0.20)$ compounds prepared by the sol-gel method.

$x = 0.00$

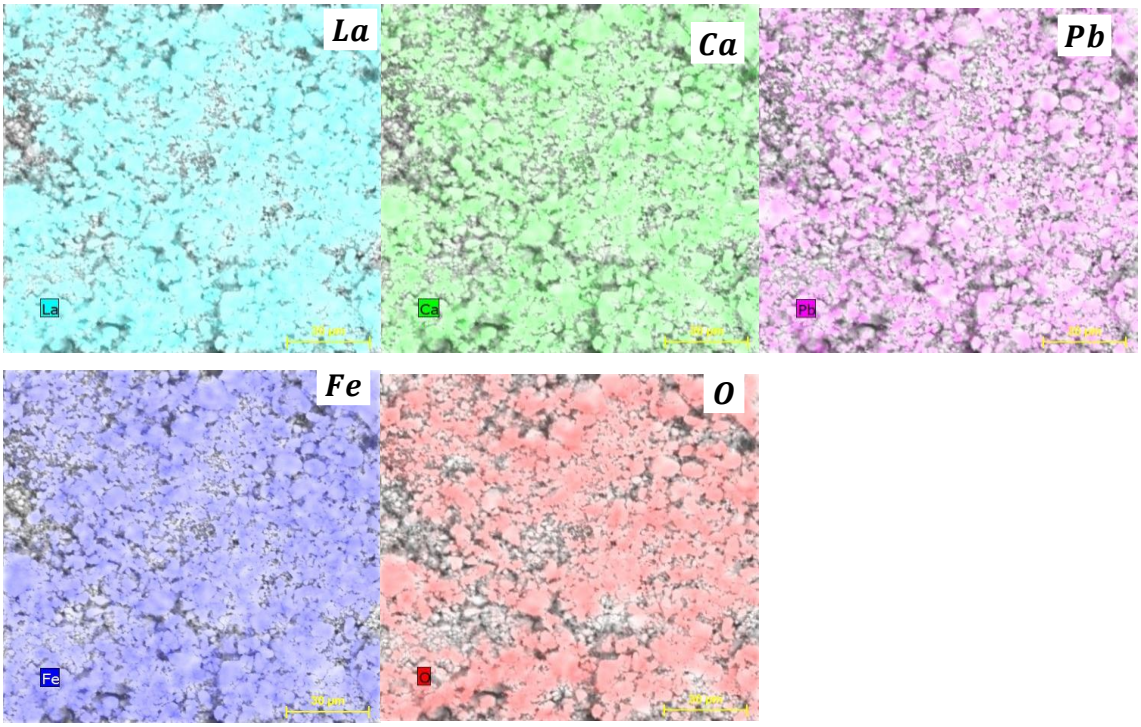

$x = 0.10$

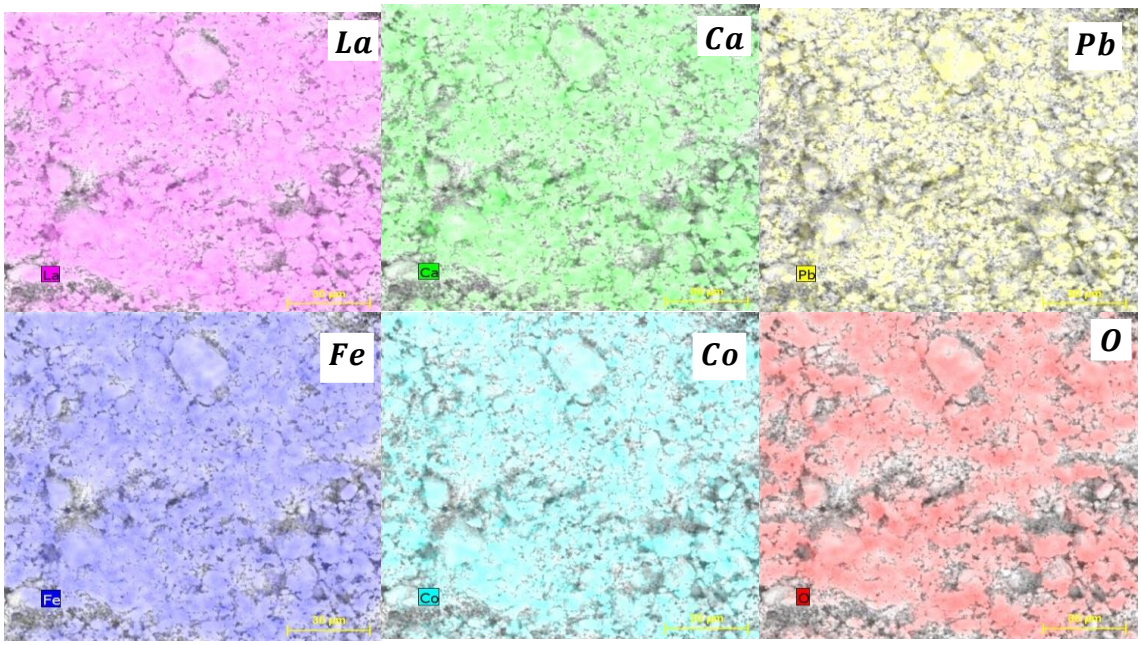

Figure. 4 (*b*) : *EDX*-mapping of chemical elements in $La_{0.8}Pb_{0.1}Ca_{0.1}Fe_{1-x}Co_xO_3$ ($x = 0.00$ *and* $x = 0.10$) samples prepared by the sol-gel method.

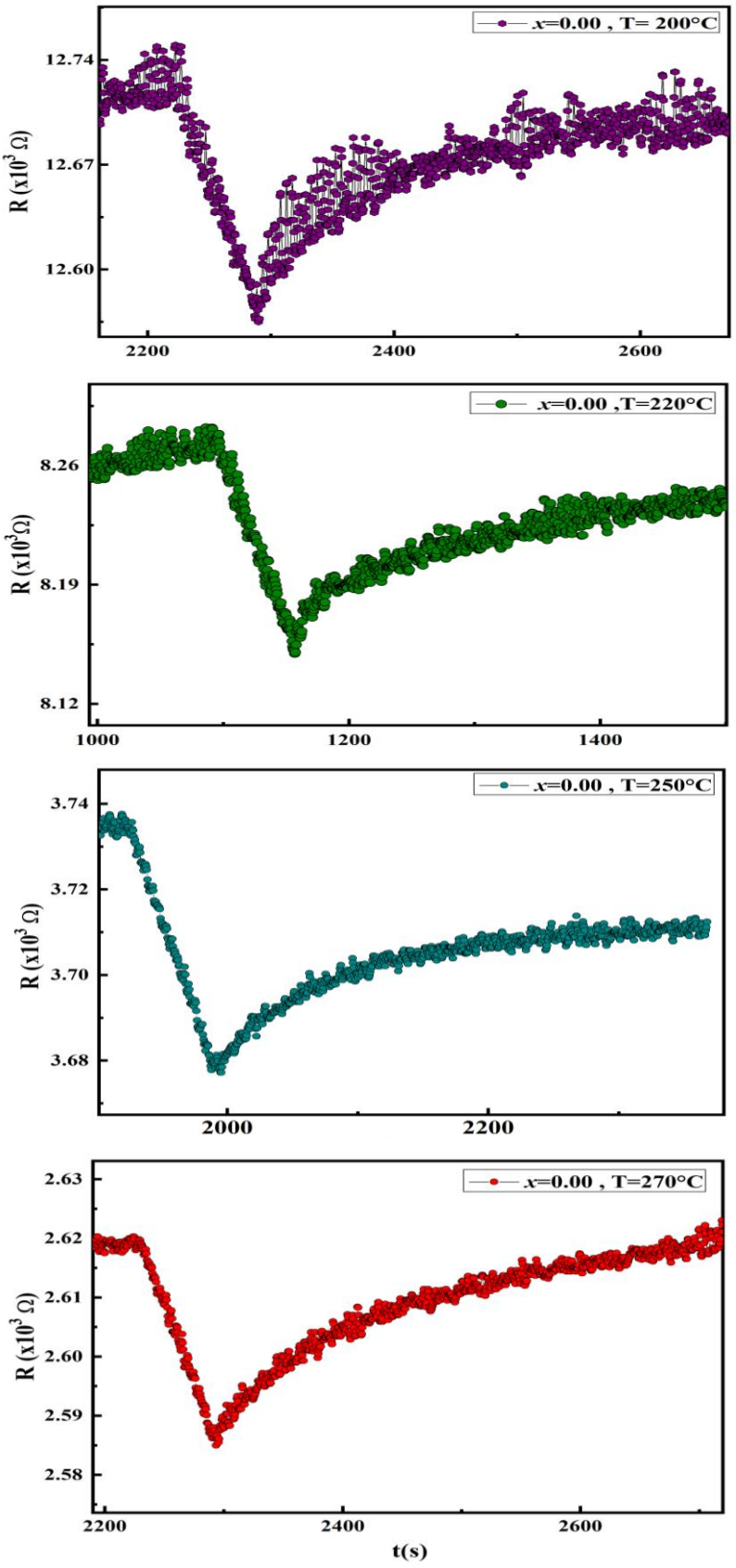

Figure. 5 (a) : Ozone gas response of $La_{0.8}Pb_{0.1}Ca_{0.1}FeO_3$ $(x = 0.00)$ sensor as a function of time at several temperatures $(200, 220, 250$ and $270\ ^{\circ}C)$.

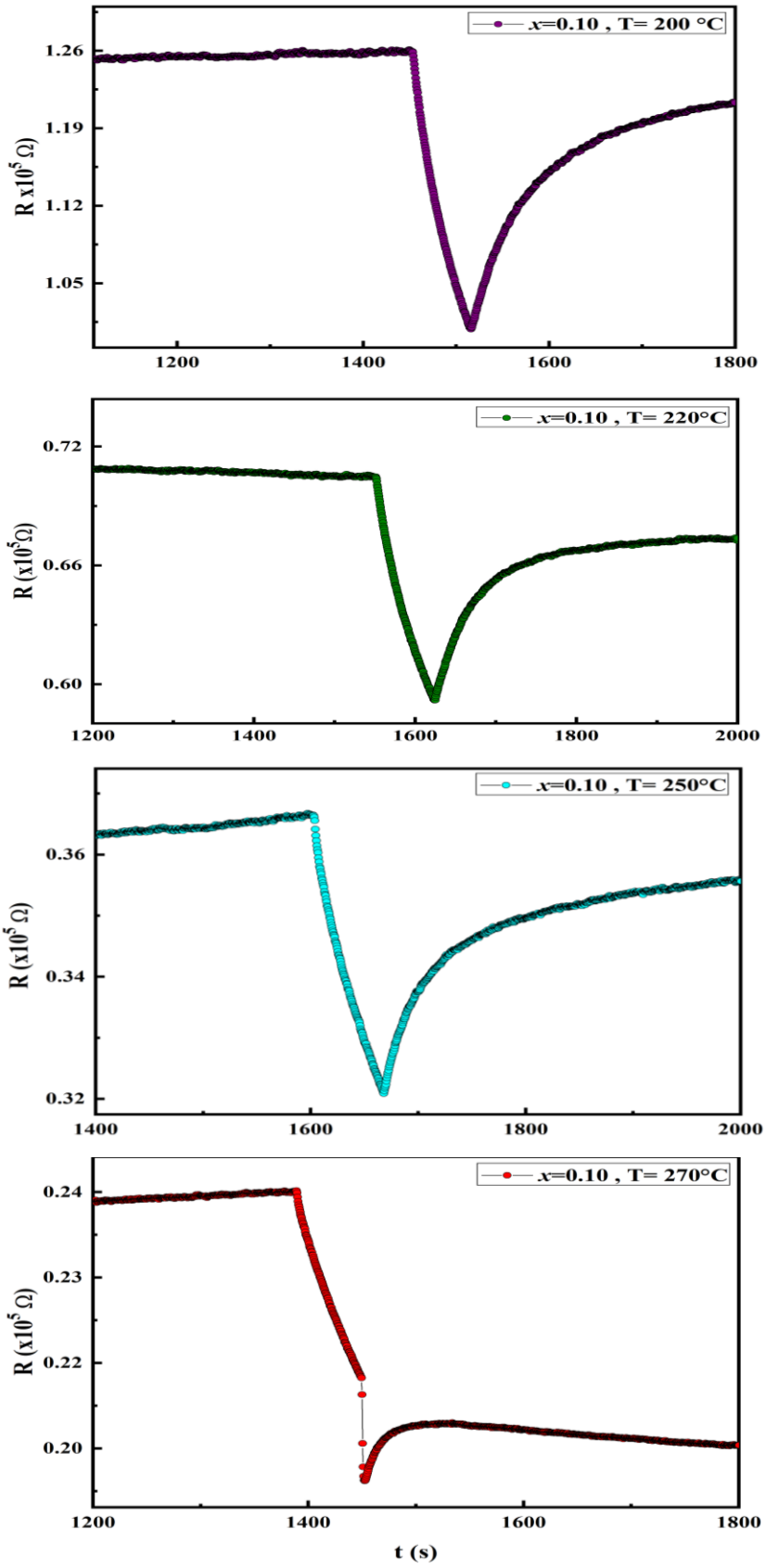

Figure. 5 (b) : Ozone gas response of $La_{0.8}Pb_{0.1}Ca_{0.1}Fe_{0.9}Co_{0.1}O_3$ $(x = 0.10)$ sensor as a function of time at several temperatures $(200, 220, 250$ and $270\ °C)$.

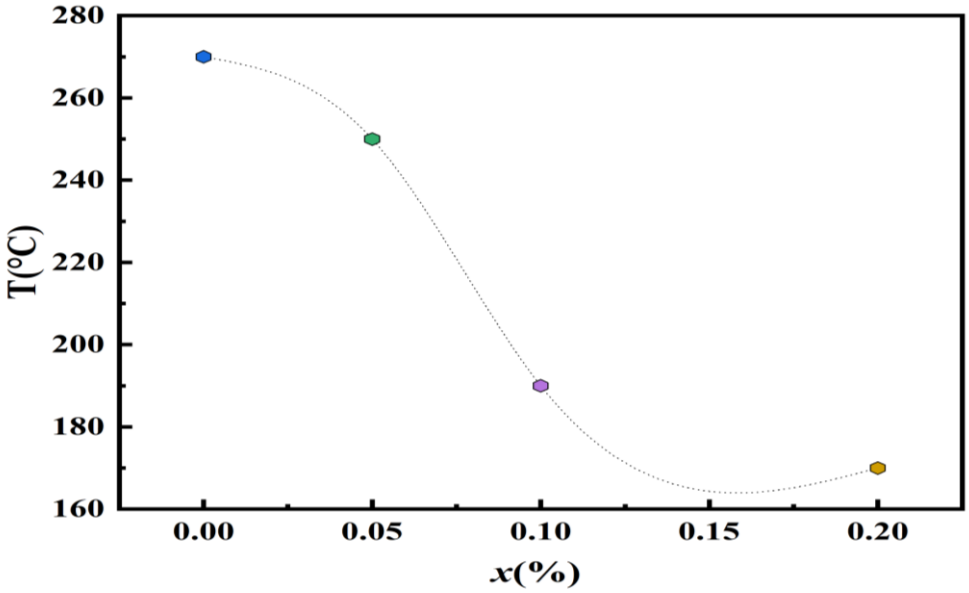

Figure. 6 : Variation of the operating temperature as a function of Co-content of $La_{0.8}Pb_{0.1}Ca_{0.1}Fe_{1-x}Co_xO_3$ ($0.00 \leq x \leq 0.20$) sensors.

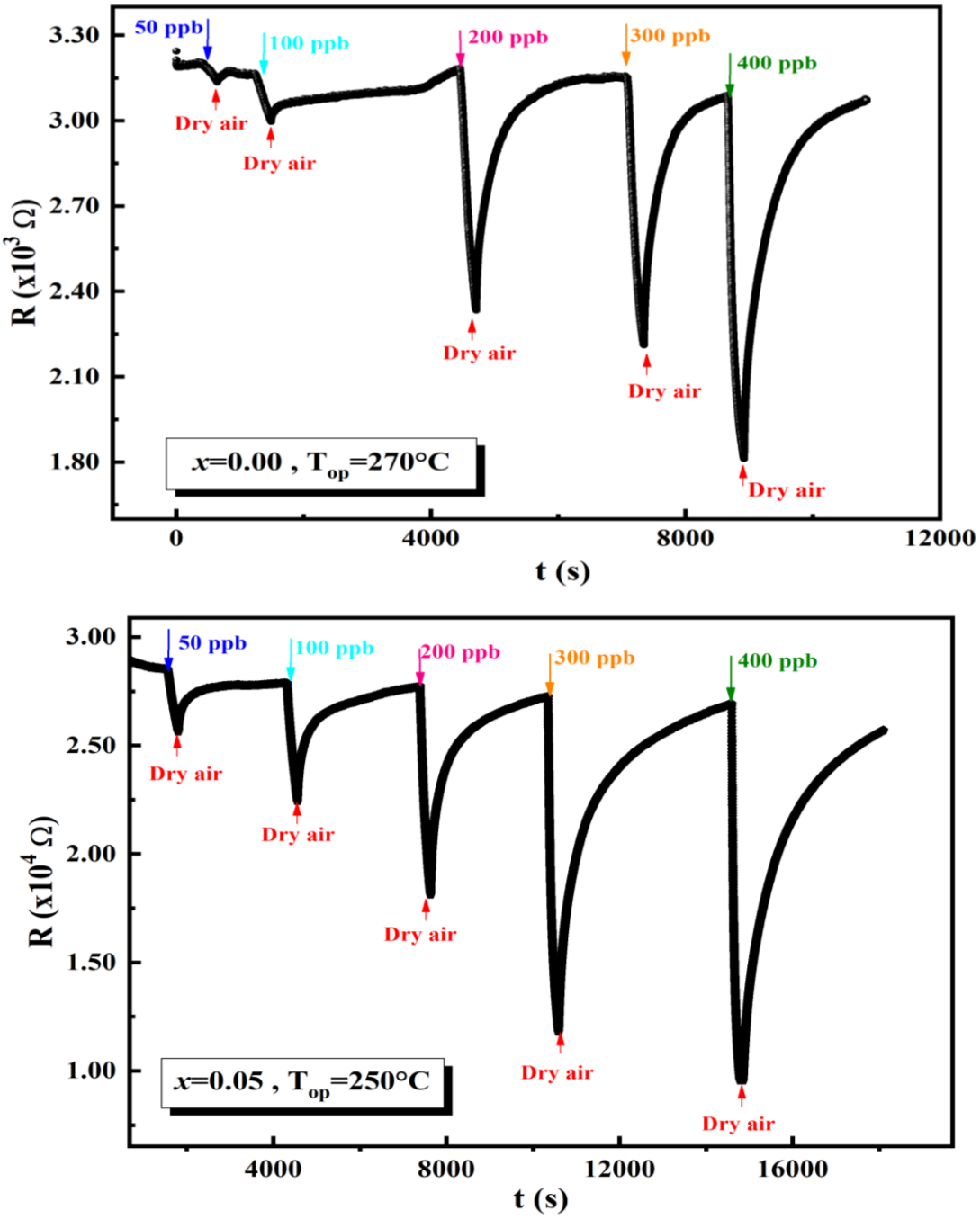

Figure. 7 : $La_{0.8}Pb_{0.1}Ca_{0.1}Fe_{1-x}Co_xO_3$ ($x = 0.00$ *and* $x = 0.05$) sensors response (S) to oxidizing gas (O_3).

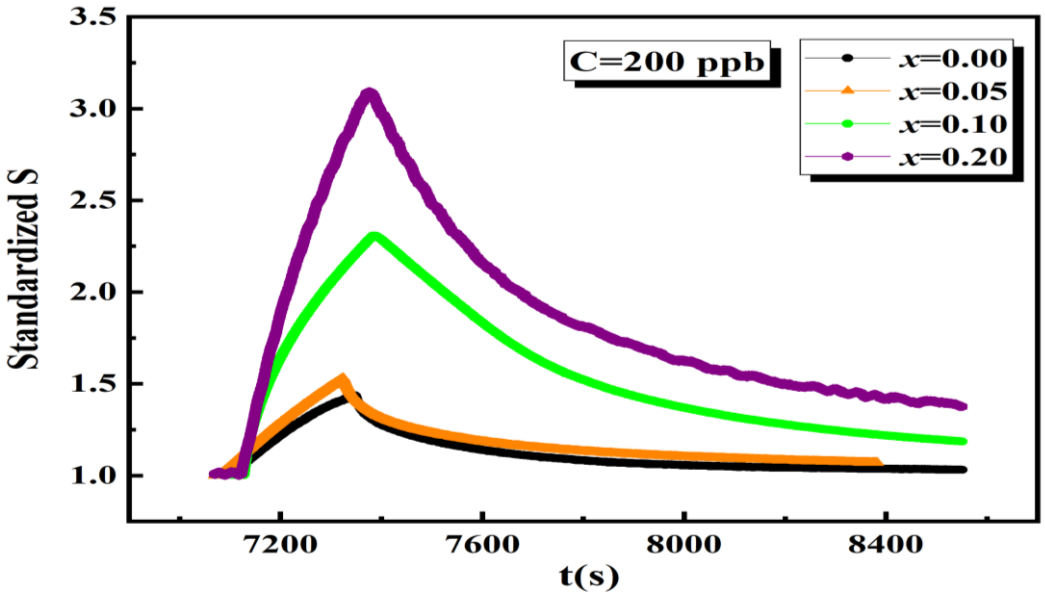

é

Figure. 8 : Ozone gas response of $La_{0.8}Pb_{0.1}Ca_{0.1}Fe_{1-x}Co_xO_3$ $(0.00 \leq x \leq 0.20)$ when sensors are exposed to 200 ppb as a function of time at the T_{op} of each sensor.

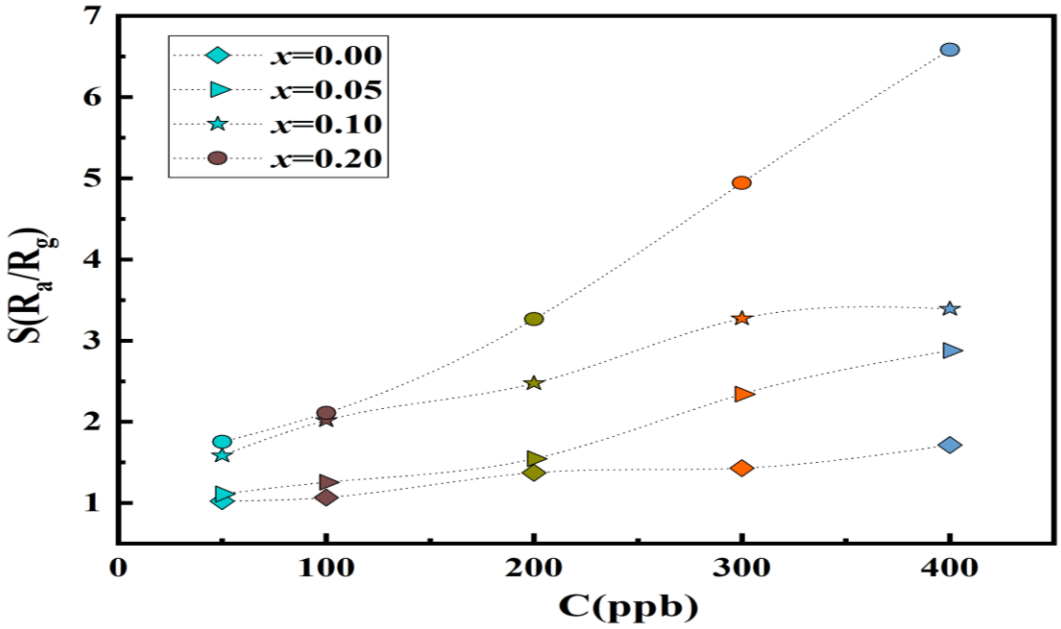

Figure. 9 : $La_{0.8}Pb_{0.1}Ca_{0.1}Fe_{1-x}Co_xO_3$ $(0.00 \leq x \leq 0.20)$ sensors responses depending on the O_3 concentrations $(50, 100, 200, 300$ and $400\ ppb)$.

References

[1] J.W. Yoon, M.L. Grilli, E.D. Bartolomeo, R. Polini, E. Traversa, The NO_2 response of solid electrolyte sensors made using nano-sized $LaFeO_3$ electrodes, J. Sens. Actuators B. Chem, **76** (**2001**) **483**.

[2] G.H. Zhang, Q. Chen, X.Y. Deng, H.Y. Jiao, P.Y. Wang, D.J. Gengzang, Synthesis and characterization of In-doped $LaFeO_3$ hollow nanofibers with enhanced formaldehyde sensing properties ,J. Mater. Lett, **236** (**2019**)**229** − **232**.

[3] B. Wang, Q. Yu, S. Zhang, T. Wang, P. Sun, X. Chuai, G. Lu, Gas sensing with yolk-shell LaFeO3 microspheres prepared by facile hydrothermal synthesis, J. Sens. Actuators B. Chem, 258 (2018)1215 − 1222.

[4] E. Cao, A. Wu, H.Wang, Y.Zhang, W.Hao, L.Sun, Enhanced Ethanol Sensing Performance of Au and Cl Comodified LaFeO3 Nanoparticles, ACS Applied Nano Materials, 2 (2019) 1541-1551.

[5] Y. Chen, H. Qin, X. Wang, L. Li, J. Hu, Acetone sensing properties and mechanism of nano-$LaFeO_3$ thick-films, J. Sens. Actuators B. Chem, 235 (2016)56 − 66.

[6]V.R. Mastelaro, S.C. Zilio, L.F.D. Silva, P.I. Pelissari, M.I.B. Bernardi, J. Guerin and K. Aguir, Ozone gas sensor based on nanocrystalline $SrTi_{1-x}Fe_xO_3$ thin films, J. Sens. Actuat. B Chem, 181 (2013) 919.

[7] K. Fan, H. Qin, L. Wang, L. Ju, J. Hu, CO2 gas sensors based on La1−xSrxFeO3 nanocrystalline powders, J. Sens. Actuators B. Chem, 177 (2013)265 − 269.

[8] Z.C. Xu, M.F. Liu, C.C. Chen, X.N. Ying, Charge disproportionation in La1-xCaxFeO3−δ (x = 0.4 and 0.5) investigated by mechanical spectroscopy,J. Appl. Phy, 115 (2014) 123516.

[9] L.S.R. Rocha, C.R.Foschini, C.C.Silva, E.Longo, A.Z.Simões, Novel ozone gas sensor based on ZnO nanostructures grown by the microwave-assisted hydrothermal route
J. Ceram. Int, 42 (2016) 4539 − 4545.

[10] M. Mori, Y. Itagaki, Y. Sadaoka, Effect of VOC on ozone detection using semiconducting sensor with SmFe1−xCoxO3 perovskite-type oxides, J. Sens. Actuators B. Chem, 44 (2012) 163.

[11] R. Köferstein, L. Jäger, S. Ebbinghaus, Magnetic and optical investigations on LaFeO3 powders with different particle sizes and corresponding ceramics, J. solid State Ionics, 249 (2013) 1-5.

[12] N. Rezlescu, E. Rezlescu , P. D. Popa, C. Doroftei, M. Ignat, Characterization and catalytic properties of some perovskites, J. Composites, 60 (2014) 515-522.

[13] A. A. Alharbi, A. Sackmann, U. Weimar, N. Barsan, Acetylene- and Ethylene-Sensing Mechanism for $LaFeO_3$-Based Gas Sensors: Operando Insights, J. Phys. Chem C, 124 (2020) 7317-73263.

[14] A. Benali, M. Bejar, E. Dhahri , M. Sajieddine , M.P.F. Graça, M.A. Valente, Magnetic, Raman and Mössbauer properties of double-doping $LaFeO_3$ perovskite oxides, J. mater. Chem. Phys, 149 (2015)467-472.

[15] P. Song, H. Qin, L. Zhang, K. An, Z. Lin, J. Hu, M. Jiang, The structure, electrical and ethanol-sensing properties of La1−xPbxFeO3 perovskite ceramics with x ≤ 0.3, J. Sens. Actuators B. Chem, 104 (2005) 312-316.

[16] L. Kong, Y. Shen, Gas-sensing property and mechanism of $Ca_xLa_{1-x}FeO_3$ ceramics, J. Sens. Actuators B. Chem, 30 (1996)217 − 221.

[17] P. Song, J. Hu, H. Qin, L. Zhang, K. An, Preparation and ethanol sensitivity of nanocrystalline La0.7Pb0.3FeO3-based gas sensor, J. Mat. Lett, 58 (2004) 2610.

[18] S. Smiy, H. Saoudi, A. Benali, M. Bejar, E. Dhahri, T. Fiorido, M. Bendahan, K. Aguir, Correlation between structural, magnetic and gas sensor properties of $La_{0.885}Pb_{0.005}Ca_{0.11}Fe_{1-x}Co_xO_{2.95}$ ($0.00 \leq x \leq 0.15$) compounds, J. Mater. Res. Bull, 130 (2020) 110922.

[19] H. Saoudi, A. Benali, M. Bejar, E. Dhahri, T. Fiorido, K. Aguir, R. Hayn, Structural and NH3 gas-sensing properties of La0.8Ca0.1Pb0.1Fe1-xCoxO3 (0.00 ≤ x ≤ 0.20) perovskite compounds, J. Alloys. Compds, 731(2018) 655.

[20] H.Y. Li, C.S. Lee, D. H. Kim and J.H. Lee, Flexible Room-Temperature NH3 Sensor for Ultrasensitive, Selective, and Humidity-Independent Gas Detection, J. ACS Appl. Mater. Interfaces, 10 (2018) 27858−27867.

[21] F.L.Pennec, A.E.Halabi, S.Bernadini, C.P.Pellegrino, K.Aguir, M.Bendahan, CO2 detection by barium titanate deposited by drop coating and Screen-Printing Methods, International journal on Advances in systems and measurements, 13 (2020) 333-341.

[22] S. Smiy, H. Saoudi, A. Benali, M. Bejar, E. Dhahri, T. Fiorido, K. Aguir, New perovskite compound La0.885Pb0.005Ca0.11FeO2.95 for gas sensing application, J. Chem. Phys. Lett, 735 (2019) 136765.

[23] A. Benali, S. Azizi, M. Bejar, E. Dhahri, M.F.P. Graça, Structural, electrical and ethanol sensing properties of double-doping LaFeO3 perovskite oxides, J. Ceram. Int, 40 (2014) 14367.

[24] T. Addabbo, F. Bertocci, A. Fort, M. Gregorkiewitz, M. Mugnaini, R. Spinicci, V. Vignoli, Gas sensing properties and modeling of $YCoO_3$ based perovskite materials, J. Sens. Actuators B. Chem, 221 (2015) 1137.

[25] S. Smiy, M. Bejar, E. Dhahri, T. Fiorido, K. Aguir, V.M. Laithier, M. Bendahan, Film-thichness influence on ozone detection of La0.8Pb0.1Ca0.1Fe1-xCoxO3 based sensors, New journal of chemistry, (**2021**) , DOI: 10.1039/D1NJ01368H.

[26] X. Liu, B. Cheng, J. Hu, H. Qin, M. Jiang, Semiconducting gas sensor for ethanol based on $LaMg_xFe_{1-x}O_3$ nanocrystals,J. Sens. Actuators B. Chem, **129** (**2008**)**53** − **58**.

[27] U. Pulkkinen, T.T. Rantala, T.S. Rantala, V. Lantto, Kinetic Monte Carlo Simulation of Oxygen Exchange of SnO_2 Surface, J. Mol. Catal A. Chem, 166 (2001) 15.

[28] S. Xu, Y. Yang, C. Jiang, J. Gao, L. Jing, P. Shen, L. Li, K. Shi, Enhanced NH_3 gas sensing performance based on electrospun alkaline-earth metals composited SnO_2 nanofibers , J. Alloys. Compds, 618 (2015) 240.

[29] S. Smiy, M. Bejar, E. Dhahri, T. Fiorido, M. Bendahan, K. Aguir, Ozone detection based on nanostructured La0.8Pb0.1Ca0.1Fe0.8Co0.2O3 thin films, J. Alloys. Compds, **829** (**2020**) **154596**.

[30] J. Guerin, M. Bendahan, K. Aguir, A dynamic response model for the WO_3-based ozone sensors, J. Sens. Actuators B. Chem, **128** (**2008**)**462** − **467**.

[31] V.R. Mastelaro, S.C. Zilio, L.F.D. Silva, P.I. Pelissari, M.I.B. Bernardi, J. Guerin, K. Aguir, Ozone gas sensor based on nanocrystalline $SrTi_{1-x}Fe_xO_3$ thin films, J. Sens. Actuators B. Chem, **181** (**2013**)**919** − **924**.

[32] Bulletin of Alloy Phase Diagrams, 10 (1989) 370.

[33] A. Gurlo, N. Barsan, M. Ivanovskaya, U. Weimar and W. Göpel, In_2O_3 and MoO_3–In_2O_3 thin film semiconductor sensors: interaction with NO_2 and O_3, J. Sens. Actuators B. Chem, **47** (**1998**) **92**.

[34] W. Qu and W. Wlodarski, Immunoassay systems based on immunoliposomes consisting of genetically engineered single-chain antibody, J. Sens. Actuators B. Chem, 64 (2000) 42-45.

[35] T. Sathiwitayakul, E. Newton, I. P. Parkin, M. Kuznetsov and R. Binions, Ferrite materials produced from self-propagating high-temperature synthesis for gas sensing applications, J. IEEE Sens, 15 (2015)196 − 200.

[36] A. Gaddari, F. Berger, M. Amjoud, J.B. Sanchez, M. Lahcini, B. Rhouta, D. Mezzane, C. Mavon, E. Beche and V. Flaud, A novel way for the synthesis of tin dioxide sol–gel derived thin films: application to O_3 detection at ambient temperature, J. Sens. Actuat. B Chem, 176 (2013) 811.

[37] A. Bejaoui, J. Guerin, J.A. Zapien and K. Aguir, Theoretical and experimental study of the response of CuO gas sensor under ozone, Sensors and Actuators B, 190 (2014) 8.

[38] L. Shoa, Z. Wu, H. Duan and T. Shaymurat, Discriminative and rapid detection of ozone realized by sensor array of Zn^{2+} doping tailored MoS_2 ultrathin nanosheets, J. Sens. Actuat. B Chem, 258 (2018) 937.

[39] R. Waser, Nanoelectronics and Information Technology: Advanced Electronic Materials and Novel Devices, Wiley-VCH, Weinheim, Germany (2005).

[40] M. Mori, J. Fujita, Y. Itagaki and Y. Sadaoka, Ozone detection in air using $SmFeO_3$ gas sensor for air quality classification, J. Cera. Soc. Japan, 119 (2011) 926.

[41] P.C. Chou, H.I. Chen, I.P. Liu, C.C. Chen, J.K. Liou, K.S. Hsu, and W.C. Liu, On the ammonia gas sensing performance of a RF sputtered NiO thin-film sensor, J. IEEE. Sens, 15 (2015)3711 − 3715.

[42] H.I. Chen, C.Y. Hsiao, W.C. Chen, C.H. Chang, T.C. Chou, I.P. Liu, K.W. Lin and W.C. Liu, Characteristics of a Pt/NiO thin film-based ammonia gas sensor, J. Sens. Actuators B. Chem, 256 (2018) 962.